Pergamon

SCIENCE DIRECT®

Bioorganic & Medicinal Chemistry 11 (2003) 2783–2790

BIOORGANIC & MEDICINAL CHEMISTRY

Detection of Acceptor Sites for Antisense Oligonucleotides on Native Folded RNA by Fluorescence Spectroscopy

Atsushi Mahara,[a] Reiko Iwase,[a] Takashi Sakamoto,[a] Tetsuji Yamaoka,[a] Kazushige Yamana[b] and Akira Murakami[a,*]

[a]*Department of Polymer Science and Engineering, Kyoto Institute of Technology, Matsugasaki, Kyoto 606-8585, Japan*
[b]*Department of Applied Chemistry, Himeji Institute of Technology, Shosha, Himeji, Japan*

Received 27 January 2003; accepted 31 March 2003

Abstract—Antisense strategy has high potential for curing diseases and studying gene functions by suppressing the translation step. For the strategy, it is essential to detect acceptor sites of antisense molecules on mRNA under physiological conditions. We propose a new analytical method for the detection of acceptor sites of antisense molecules with high sensitivity. 2′-*O*-Methyloligoribonucleotide containing 2′-*O*-(1-pyrenylmethyl)uridine (OMUpy) was chosen as the fluorescence probe. The fluorescence intensity due to the pyrene in single-stranded OMUpy was scarcely observed. When OMUpy was hybridized with the complementary oligoRNA, the fluorescence intensity at 375 nm was remarkably increased. It was found that the increase was derived from the localization of the pyrene by the measurements of time-resolved fluorescence spectroscopy, CD and UV absorption spectra. These results suggest that the change of the fluorescence intensity of OMUpy can be a useful index to monitor hybridization. In this study, we chose *Escherichia coli*. 16S-rRNA as the model RNA and chose seven regions for probing by OMUpy based on the reported secondary structure of 16S-rRNA. The fluorescence intensity of an equimolar mixture of OMUpy with 16S-rRNA varied depending on the sequence. In particular, the increment in the system of OMUpy-8, which can hybridize with region 887–896 nt of 16S-rRNA, was most significant among the systems. These results indicated that the site targeted by OMUpy-8 was exposed to regulatory molecules, and suggest that the method presented here is useful to design antisense molecules.
© 2003 Elsevier Science Ltd. All rights reserved.

Introduction

Recently, antisense strategy has attained reality in curing diseases such as cytomegalovirus, HIV, and various types of cancers. The strategy also has high potential for studying gene functions by suppressing the translation step. Actually, the strategy intrinsically has some problems. They are as follows: (a) cellular uptake efficiency, (b) stability in the cytoplasm, (c) acute and chronic toxicity, (d) ability for RNase H activation, (e) reasonable sequence determination protocol. Among the problems, the most important issue is to select the region that can accept antisense molecules.[1] Messenger RNA (mRNA) has a native folded structure under physiological conditions and various types of cellular proteins interact with mRNA in the cytoplasm. These features probably prevent the antisense molecules from binding with the target mRNA. By now, various trials to detect such regions on mRNA have attained partial success. Gel electrophoresis estimation,[2] DNA-chip or DNA-array methodology[3,4] and computer-aided modeling of RNA structures[5–7] have been developed. Because of the simple manipulation, these methods are highly effective in the detection of antisense molecules. On the other hand, fluorescence methods have been utilized to detect a target sequence and to analyze the interaction between biomolecules under physiological conditions. One of the most useful methods is based on fluorescence resonance energy transfer (FRET). The molecular beacon based on FRET is widely used for the detection of target RNA and DNA.[8,9] As another method, fluorescence anisotropy analysis was adopted to detect the acceptor sites on RNA using a fluorescein-conjugated oligonucleotide.[10] Also, various types of pyrene-labeled oligonucleotides have been investigated for the detection of target sites.[11–16] In these fluorescence methods, it is important to discriminate the fluorescence signal of the hybrid from that of the non-binding probes. In this study, we apply the fluorescent-labeled oligonucleotide to detect acceptor sites on biomolecules where RNA-regulating molecules such as antisense molecules can react. We have been studying fluorescent DNA

*Corresponding author. Tel.: +81-75-724-7814; fax: +81-75-724-7814; e-mail: akiram@ipc.kit.ac.jp

0968-0896/03/$ - see front matter © 2003 Elsevier Science Ltd. All rights reserved.
doi:10.1016/S0968-0896(03)00227-X

probes that can enhance fluorescence only when they specifically interact with the target mRNA. The probe should discriminate the hybrid with RNA from the single-stranded probe under homogenous conditions.

In our previous work, we have reported a pyrene-labeled DNA probe, which enhanced its fluorescence upon hybridization with complementary oligoribonucleotides (ORN) up to about 250-fold but not with complementary oligodeoxyribonucleotides.[17] The enhancement of the pyrene is probably derived from the change of the environment of the pyrene. However, the fluorescence intensity of the hybrid of pyrene-labeled DNA probe with RNA is about 1% compared with that of 1-pyrenylmethanol, and the excitation energy of the pyrene is still quenched by adjacent nucleotide bases. If the excitation energy is completely converted to the fluorescence emission only when hybridized with the target RNA, the high sensitive probe could be developed for the detection of RNAs. Furthermore, we also focus on the future usage in living cells. For the purpose, it is required that the probe should be stable in the cytoplasm and that it should not stimulate RNase H. Furthermore, the probe needs to form a stable hybrid with the target RNA. Based on these points of view, we developed a pyrene-labeled 2′-*O*-methyloligonucleotide (OMUpy) as the probe for the RNA detection. Recently, bispyrene-conjugated 2′-*O*-methyloligoribonucleotides (OMUpy2) were synthesized and fluorescence property of the OMUpy2 was investigated.[18] The fluorescence emission of the single-stranded OMUpy2 was scarcely observed. When the OMUpy2 was hybridized with oligo-RNA, the broad structureless emission around 480 nm was increased to 43.7-fold as compared with that of single-stranded OMUpy2. However, the increase of fluorescence emission about the OMUpy2 was smaller than that of pyrene-labeled DNA probe. In order to detect the binding sites of antisense molecules in detail and quantitatively, the improvement of the probe is essential.

This report presents the spectroscopic characterization of OMUpy that can detect the binding site of antisense molecules on native folded RNAs. In order to estimate the detection of the binding sites, we also adopt a 16S ribosomal RNA as a target one whose secondary and tertiary structures have been reported,[19–21] because there is little information about mRNA in the physiological conditions.

Results and Discussion

We have previously reported that oligodeoxyribonucleotides (Upy-Oligo) containing 2′-*O*-(1-pyrenylmethyl)uridine (Upy) are characteristic fluorescent probes to discriminate RNA from DNA.[17,22] The fluorescence intensity of Upy-Oligo drastically increased to 248-fold upon hybridization with its complementary oligoribonucleotides (cORN) but did not with complementary oligodeoxyribonucleotides (cODN). These results inspired us to use the probe to specify the acceptor regions of antisense DNA in target RNAs under physiological conditions, where RNAs spontaneously form their native folded structure. Various trials have finally led us to adopt OMUpy. 2′-*O*-Methylation of oligoribonucleotides endows antisense molecules with several interesting features as follows; greater ability for hybrid formation, no susceptibility to RNase H, and relatively higher stability under in vivo conditions.[23] Those features fulfill the requirements for the further purpose to use the pyrene probe in vivo.[24] UpyC was chosen according to the previous studies from four sequences, -UpyX- (X: A, G, T, C), and introduced to 2′-*O*-methyloligoribonucleotide (OMUpy, Fig. 1, Table 1).

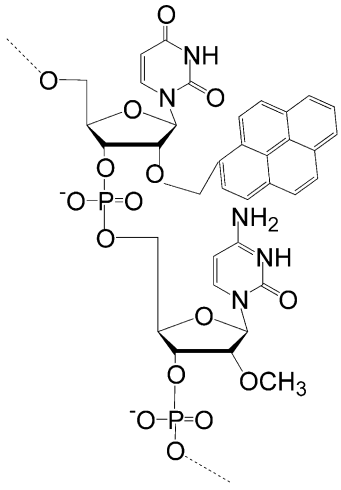

Figure 1. Structure of pyrene-conjugated 2′-*O*-methyloligoribonucleotide (OMUpy).

Table 1. Sequence of the probe and *T*m value of the duplex with cORN

Abbreviation	Target RNA	Sequence	Target site	Molecular weight[a]		T_m (°C)[b]
				Calculated *m*/*z*	Found *m*/*z*	
OMUpy-1	5S-rRNA	5′-GU**Upy**CGGCAUG-3′	38–47 nt	3517.5	3518.6	47.4
OMUpy-2	16S-rRNA	5′-CAGCGU**Upy**CAA-3′	29–38 nt	3483.3	3482.8	45.0
OMUpy-3	16S-rRNA	5′-A**Upy**CUGGGCAC-3′	230–239 nt	3499.3	3500.0	56.7
OMUpy-4	16S-rRNA	5′-GUA**Upy**CAGAUG-3′	634–643 nt	3524.3	3524.5	35.5
OMUpy-5	16S-rRNA	5′-UGAA**Upy**CACAA-3′	1471–1480 nt	3491.3	3492.0	28.0
OMUpy-6	16S-rRNA	5′-CCGUG**Upy**CUCA-3′	323–332 nt	3436.3	3437.4	48.1
OMUpy-7	16S-rRNA	5′-CAGUAAU**Upy**CC-3′	557–566 nt	3444.3	3444.4	38.5
OMUpy-8	16S-rRNA	5′-GCCGUAC**Upy**CC-3′	887–896 nt	3435.3	3435.9	58.4

[a]Molecular weight was confirmed by MALDI-TOF MS analysis.
[b]Melting temperatures were calculated by UV melting curves. Detailed conditions were described in Material and methods.

Fluorescence properties of single-stranded OMUpy

Prior to the application of OMUpy to the native folded RNA study, the behavior of the electronic spectra of pyrene in OMUpy was studied in detail. Fluorescence spectra of single-stranded OMUpy-1 and 1-pyrenylmethanol in an aqueous medium are shown in Figure 2. The fluorescence intensity of OMUpy-1 was about 0.1% that of 1-pyrenylmethanol, suggesting that the emission of the pyrene in OMUpy-1 was largely quenched and the property was the same as that of pyrene-labeled DNA. To investigate the environment of the pyrene in OMUpy, the UV-absorption and circular dichroism (CD) spectra of OMUpy-1 were measured. Figure 3 shows the UV-absorption spectra of 1-pyrenylmethanol, single-stranded OMUpy-1 and an equimolar mixture of OMUpy-1 and cORN (or cODN). The absorbance of OMUpy-1 around 300–380 nm decreased to 65% compared to that of 1-pyrenylmethanol, and the wavelength of the maximal absorption was red-shifted by 9 nm. It is likely that the transition moment of the pyrene in single-stranded OMUpy interacted with those of adjacent nucleotide bases. Therefore, it is probable that fluorescence quenching of the pyrene and the red shift in UV absorption spectra are both due to the stacking interaction between pyrene and the nucleotide bases. Moreover, the CD spectra of single-stranded OMUpy-1 was measured and as shown in Figure 4, the negative signal of CD spectra around 330 nm suggested that the pyrene in single-stranded OMUpy-1 was located in the chiral environment and that the pyrene was intercalated between the adjacent uracil and cytosine. It is concluded that the quenching of the fluorescence was attributed to the excitation energy transfer from the pyrene of single-stranded OMUpy to the triplex state of uridine.

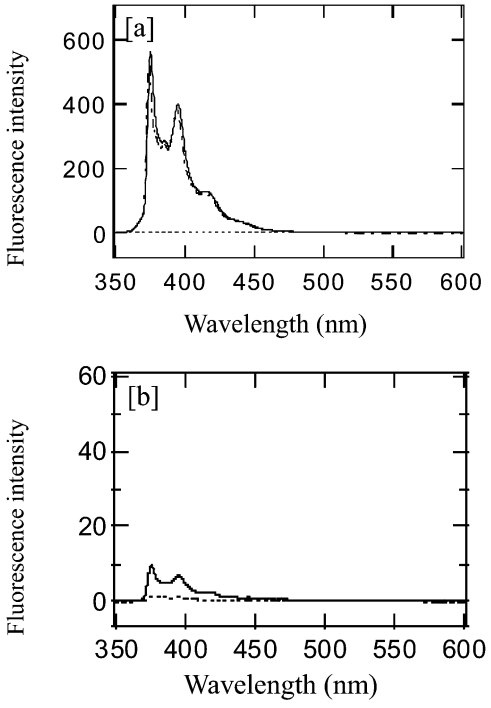

Figure 2. (a) Fluorescence spectra of 1-pyrenylmethanol (dash-dotted line), OMUpy-1 (broken line) and an equimolar mixture of OMUpy-1 with cORN (solid line); (b) fluorescence spectra of OMUpy-1 (broken line) and an equimolar mixture of OMUpy-1 with cODN (solid line). Measurements were carried out at 11 °C in 10 mM phosphate buffer and 0.1 M NaCl adjacent in pH 7.0. [OMUpy-1] = [cORN] = [cODN] = 6 μM, λ_{ex} = 342 nm.

Fluorescence properties of double-stranded OMUpy with ODN and ORN

To estimate the ability of OMUpy to form a duplex with ORN, UV melting profiles were obtained. Melting temperatures (T_m) of the duplex calculated by the results (Table 1) suggest that OMUpy can form a stable duplex with cORN under physiological conditions. Fluorescence spectra of the duplex of OMUpy with cORN or cODN are shown in Figure 2. The fluorescence intensity of OMUpy-1 in the presence of cORN was drastically increased by 334-fold compared to the single-stranded OMUpy-1. Because the spectrum resembled to the monomer emission of 1-pyrenylmethanol, it is suggested that the fluorescence intensity, which was once quenched by the interaction with nucleobases, recovered to a large extent. Namely, the pyrene probably relocated upon the hybrid formation to a certain environment where the excitation energy was scarcely quenched. On the other hand, the fluorescence intensity of the hybrid with cODN was scarcely changed, suggesting that the pyrene in the duplex of OMUpy-1 with cODN remained intercalated between bases. Furthermore, the fluorescence intensity of the hybrid of pyrene-labeled DNA with cORN is about 1% as compared with that of 1-pyrenylmethanol, suggesting that the excitation energy of the pyrene in the hybrid of pyrene-labeled DNA is still quenched.

In order to examine the detailed structure of the hybrid and the environment of the pyrene, CD spectra were measured and are shown in Figure 4. The CD spectra of oligonucleotides around 260 nm reflected the interaction between the transition moments of nucleotide bases. When OMUpy-1 was hybridized with cORN, the CD spectrum around 260 nm is very similar to that of the duplex of unmodified 2′-*O*-melthyloligoribonucleotide (2′-OMe oligoRNA) with cORN. It is reported that the

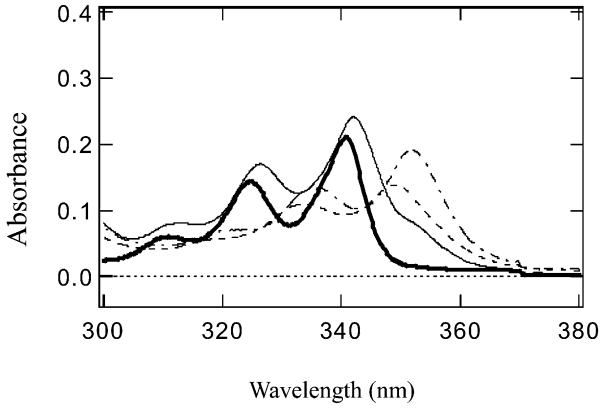

Figure 3. UV absorption spectra of 1-pyrenemethanol (solid line) and single-stranded OMUpy-1 (broken line) and an equimolar mixture of OMUpy-1 with cORN (thick solid line) and cODN (dash-dotted line). Detailed conditions of measurement were described in Material and methods.

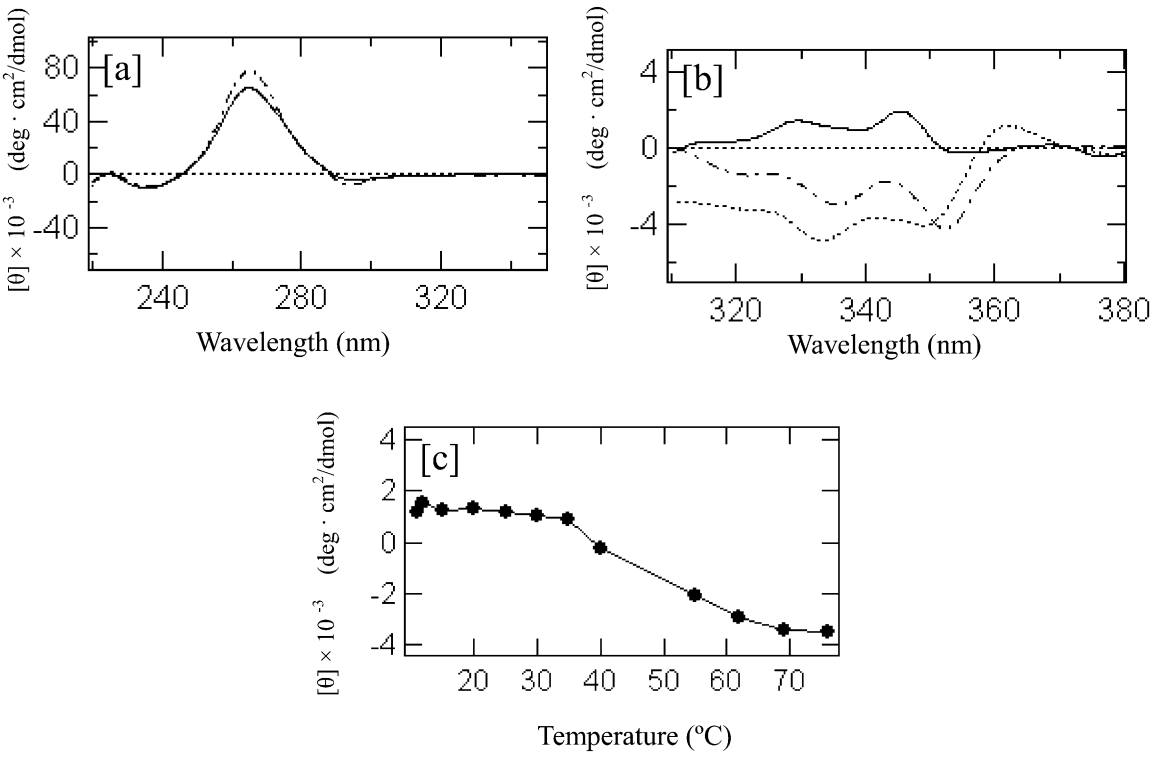

Figure 4. (a) CD spectra of the duplex of 2′-OMe oligoRNA with cORN (dash-dotted line) and the duplex of OMUpy-1 with cORN (solid line); (b) expanded CD spectra of single-stranded OMUpy-1 (dash line), the duplex of OMUpy-1 with cORN (solid line) and cODN (dash-dotted line); (c) temperature dependence of ICD at 345 nm of the duplex of OMUpy-1 with cORN. Measurements were carried out at 11 °C in the 10 mM phosphate buffer adjacent to pH 7.0. Detailed conditions were described in Material and methods.

duplex of 2′-OMe oligoRNA with cORN formed an A-form-like helix as judged by the CD[23] and by NMR spectroscopy.[25] Therefore, it seems that the duplex of OMUpy with cORN forms an A-like structure.

The CD spectra around 340 nm, which is regarded as the induced CD (ICD), were examined, which was probably induced by the coupling between the transition moments of the pyrene and that of the chirally arranged nucleotide bases. The sign of the ICD of the duplex of OMUpy-1 with cORN was positive. On the other hand, the sign of the ICD of single-stranded OMUpy-1 was negative. Moreover, the temperature dependence of ICD showed a sigmoidal curve as shown in Figure 4. It is likely that the change in the ICD signal correlated with the environmental shift of the pyrene. It is reported that the ICD around 340 nm of the duplex of benzo[*a*]pyrene-conjugated ODN with cODN could correlate with the groove binding mode of benzo[*a*]pyrene.[26] Though the negative ICD correlated only with an intercalation mode, the positive ICD correlated both with an external binding mode and with an intercalation one. These observations suggest that the pyrene of OMUpy relocated from an intercalation mode to an external binding one when hybridized with cORN. Moreover, the change in the ICD around 340 nm was not observed when OMUpy-1 was hybridized with cODN. In the case of pyrene-labeled DNA, the drastic change in ICD of pyrene is not observed. From these results, it is likely that the drastically change of the environment of pyrene in the hybrid is essential for the large increase of fluorescence intensity.

The hypothesis was supported by analysis of the fluorescence decay curve. The decay curve of OMUpy-1 showed that one fluorescent species with lifetimes of 1–3 ns substantially existed in the OMUpy-1 solution. The decay curve of the equimolar mixture of OMUpy-1 and cODN showed that two species existed with lifetimes as summarized in Table 2. The major fluorescent species with a lifetime of 1 ns accounted for ca. 98 mol%. In contrast, when cORN was present in the OMUpy-1 system, the decay curve showed a single component. The lifetime was nearly equal to that of 1-pyrenylmethanol under the same conditions. (123 ns). These results clearly suggest that two characteristic fluorescent species exist in the solution of OMUpy-1 and that the change in fluorescence intensity might be related to the ratio of the species.

To specify the detailed location of the long-lifetime species, the peak ratio of vibronic bands of the fluorescence spectra, called HAM bands, was examined. The fluorescence intensities at 375 nm (Band I) and 384 nm

Table 2. Fluorescence lifetime of OMUpy-1 and the duplex with cODN and cORN

Sample	Fluorescence lifetime (ns)				
	τ_1	f_1	τ_2	f_2	χ^2
1-Pyrenemethanol	123	0.83	38	0.17	1.01
OMUpy-1	0.9	N.D.	3	N.D.	1.52
OMUpy-1 + cODN	1.3	0.98	94	0.02	1.85
OMUpy-1 + cORN	137	1.0	—	—	1.07

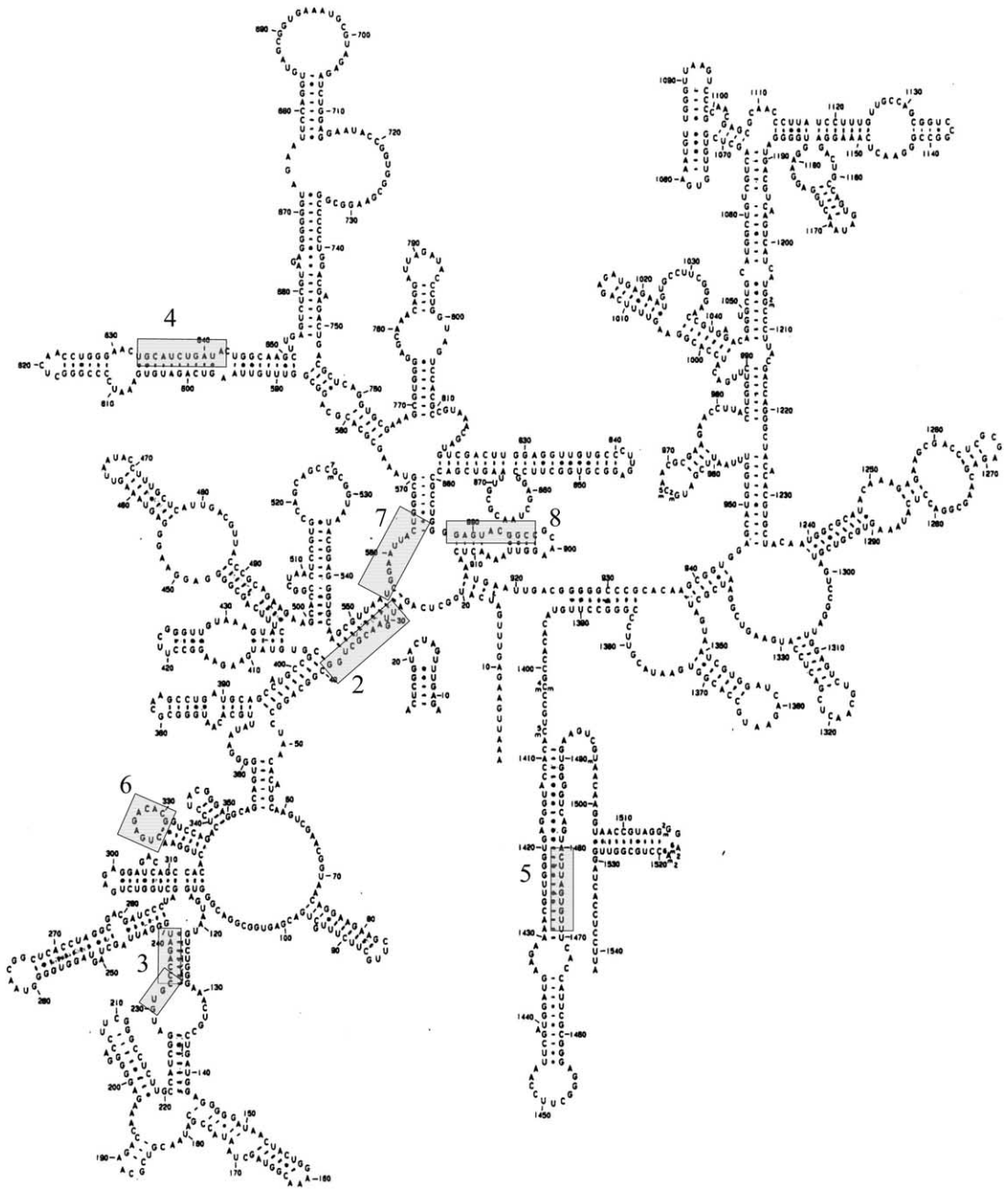

Figure 5. Secondary structure of *E. coli*. 16S-rRNA[19] and target sites of OMUpy.

(Band III) are affected by the dielectronic constant of the surrounding solvent.[27] The peak ratio of Band I/Band III of pyrene in cyclohexane (dielectric constant of cyclohexane is 2.0243) was 0.62 and that in aqueous media (dielectric constant of water is 80.1) was about 1.72. Namely, the peak ratio can represent the dielectric constant of the surrounding environment. The HAM band ratio of OMUpy-1 changed from 1.07 to 1.99 upon hybrid formation with cORN indicating that the pyrene relocated from the hydrophobic environment to the hydrophilic one. Because the dielectric constant (1.99) around the pyrene calculated from the peak ratio was similar to that of water, it seems that the environment of pyrene is outside the helix. It is concluded that pyrene in the hydrophilic environment is the species with the longer lifetime and that the pyrene in the hydrophobic environment was the species with the shorter lifetime. However, the detailed features of the localization of the pyrene are not clear at this stage. The study is now underway.

Application to native folded structure of RNA

Under physiological conditions, RNAs spontaneously form their native folded structure. The tertiary structure sometimes prevents RNA-binding molecules, such as antisense DNA, from binding to RNA. It has been essential to innovate an alternative method to specify where the accessible sites of mRNA for the antisense DNA exist in living cells. The results discussed above

showed that the OMUpy could present remarkable characteristics in the detection of cORN. Accordingly, we applied the characteristics of OMUpy to detect the RNA regions where antisense DNA can be hybridized. Before applying our probe to mRNA, we chose *Escherichia coli*. 16S-rRNA as the model RNAs whose structural information has been reported (Fig. 5). We designed our study based on the secondary structure demonstrated by the enzyme mapping protocol.[19] Seven regions (region-2 to region-5) were selected for the examination. Three of them (region-6 to region-8) were complementary to the single-stranded regions and the rest to the stem regions. The experiments under physiological conditions at 37 °C might provide information about the native structure. The equimolar mixture of OMUpy and 16S-rRNA also showed changes in fluorescence property as summarized in Figure 6.

The increase of the fluorescence intensity was observed in the systems of OMUpy-2, -3, -6, -7 and -8, though no change was observed in the system of OMUpy-4 and -5. In particular, the degree in the system of OMUpy-8 was larger than that of the other probe. From these results, it is possible to assume that OMUpy which targeted regions 2, 3, 6, 7 and 8 could hybridize with 16S-rRNA. In particular, the region, which was targeted by OMUpy-8, allows easy access of the antisense molecules. On the other hand, although regions 2 and -3 included some base-pairings in reported the secondary structure, the OMUpy-2 and -3 could hybridize with 16S-rRNA. One of the important factors is that the native structure has some diversity in physiological conditions. Therefore, it is probably that the increase was caused by the diversity of structure. In order to estimate the temperature-dependent diversity of the structure, the fluorescence enhancements at 375 nm of OMUpy were measured at different temperatures as shown in Figure 6. When the temperature was decreased from 37 to 11 °C, the fluorescence intensities of the systems varied depending on the regions. The increase of fluorescence intensity in the system of OMUpy-2 and -3 was scarcely observed at 11 °C. Moreover, the intensity of OMUpy-8 was largely decreased with decreasing temperature from 37 to 11 °C. On the other hand, the fluorescence intensity of OMUpy-6 was the same as that in the condition at 37 °C. From these results, the structural diversity probably depended on its region and the region-6 constantly forms the single-stranded structure. It is interesting that OMUpy-7 did not show substantial changes in fluorescence intensity in the presence of 16S-RNA. The region targeted by OMUpy-7 exhibited a single-stranded region by the reported secondary structure. Therefore, these regions might be incorporated in the tertiary structural constraint. These results suggest that OMUpy can detect the regions where the regulating molecules such as antisense DNA can be accepted by monitoring the change in fluorescence characteristics.

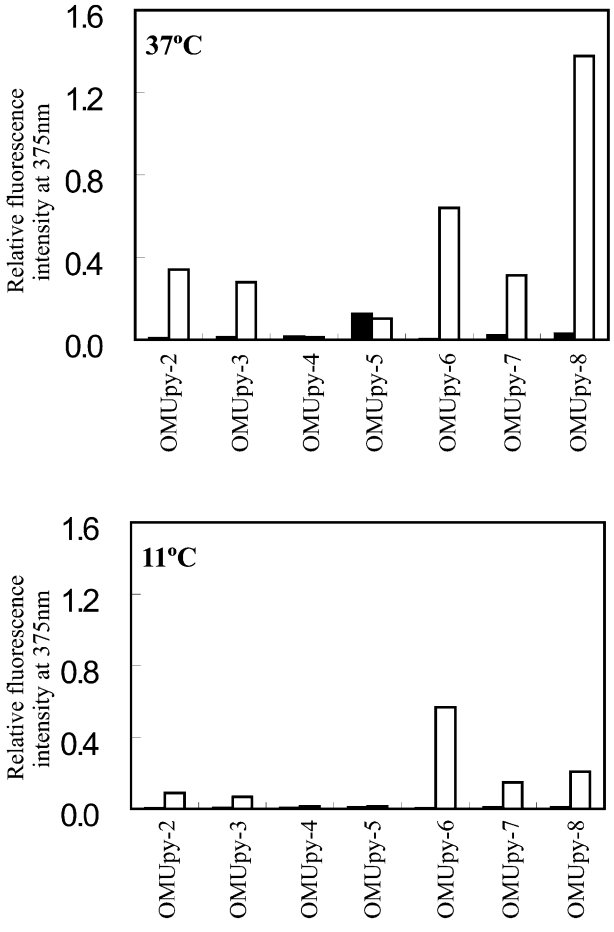

Figure 6. Relative fluorescence intensity of OMUpy1–6 in the presence (open bar) or absence (filled bar) of 16S-rRNA. Vertical axis was normalized by the intensity of the duplex of OMUpy with cORN. Measurements were carried out at 11 °C in 10 mM phosphate buffer and 0.1 M NaCl adjacent in pH 7.0. [OMUpy] = [16S-rRNA] = 0.75 μM.

Conclusion

We have studied the development of fluorescence oligonucleotide probe which can detect RNA and can discriminate RNA from DNA. In this paper, we presented a novel concept for identifying the accessible sites of RNA-regulating nucleotides on native RNA under physiological conditions. The concept presented here can be effectively applied to search for binding sites on mRNA under physiological conditions. Furthermore, the folded structure of RNA in living cells should be estimated in a real time manner. OMUpy studied in this report fulfills the fundamental requirements for the study. We recognize that two major problems exist with this probe. The one is the sequence diversity of this type of probe. In our previous studies, neither the UpyA core sequence nor the UpyU one showed any fluorescence enhancement upon hybridization with cORN. The UpyG core sequence showed 50% of the ability of the UpyC core sequence. Therefore, sequence dependence is still an unsolved problem. The improvements in this drawback are now intensively underway. Recently, we have just succeeded in synthesizing another 2′-*O*-(1-pyrenyl)nucleoside. The nucleoside should be examined similarly. The other problem is that the probe should function in living cells. For this purpose, we have chosen phosphorothioate linkages to construct the OMUpy probes. Details will be reported.

Experimental

Material

E. coli 5S ribosomal RNA and a mixture of 16S-rRNA and 23S-rRNA were purchased form Roche Diagnostic (Basel, Switzerland). 1-Pyrenemethanol and other chemical reagents were purchased form Wako Pure Chemicals (Osaka, Japan). All oligonucleotide reagents were purchased from Glen Research (Sterling, VA, USA). 2′-*O*-Methyloligonucleotides, oligodeoxyribonucleotide (ODN) and oligoribonucleotide (ORN) were synthesized using a DNA synthesizer (ABI 380, PE Biosystems) by standard phosphoramidite chemistry.

Synthesis of pyrene-conjugated OMUpy

Pyrene-conjugated OMUpy were synthesized by phosphoramidite chemistry. 5′-*O*-dimethoxytrityl-2′-*O*-(1-pyrenylmethyl)uridine-3′-*O*-(2-cyanoethyl)-*N*,*N*-diisopropylphosphoramidite (5′-DMTr-Upy amidite) was synthesized according to the reported procedure.[17] 5′-DMTr-Upy amidite was added to the pre-synthesized oligonucleotide on a CPG support followed by chain extension to the designated sequence. The pyrene-modified oligonucleotides bound to CPG were treated with 28% aqueous ammonia at 55 °C for 6 h. Purification of pyrene-modified oligonucleotides was carried out with reverse-phase HPLC with a linear gradient of acetonitrile in 0.1 M triethylammonium acetate (pH 7.0) at a flow rate of 0.8 mL/min. All pyrene-conjugated OMUpy were confirmed by MALDI-TOF MS analysis (Voyager DE-STR, Applied Biosystems).

UV absorption spectra and CD spectra measurements

Measurements of UV absorption spectra were carried out with a spectrophotometer (U-2000A, Hitachi) equipped with a thermocontrolled cell holder (SPR-10, Hitachi). Oligonucleotide solutions were prepared in a buffer containing 10 mM sodium phosphate (pH 7.0), 0.1 M NaCl. Oligonucleotide concentration was determined on the basis of the measured absorption at 260 nm using molar extinction coefficients, which were calculated by the nearest-neighbor parameters. UV-melting curves of the duplexes were obtained for solutions containing a 1:1 strand ratio of oligonucleotides with an increase in temperature from 0 to 90 °C at a rate of 1.0 °C/min. Circular dichroism (CD) spectra were obtained on a CD spectrophotometer (J-720, JASCO) equipped with a thermo controller (RET-100, Neslab). Equimolar solutions of OMUpy (6.0 μM) and corresponding oligonucleotides (6.0 μM) in the use of the measurements of CD spectra were prepared in a buffer containing 10 mM sodium phosphate (pH 7.0), 0.1 M NaCl. The measurements were carried out at 11 °C.

Fluorescence spectra measurements

Fluorescence spectra were obtained from a spectrophotometer (RF-5300PC, Shimadzu) equipped with a thermal controller. Equimolar solutions of OMUpy (0.75 μM) and corresponding oligonucleotides (0.75 μM) were denatured at 75 °C for 5 min and slowly cooled to 11 °C prior to measurements. Fluorescence spectra of the mixture of OMUpy and 5S-rRNA were obtained from a solution containing a 1:1 strand ratio of OMUpy and 5S-rRNA, which was dissolved in 10 mM sodium phosphate (pH 7.0), 0.1 M NaCl. The mixture of 16S-rRNA and 23S-rRNA was dissolved in 10 mM Tris buffer (pH 7.4), 1 mM $MgCl_2$, and 0.1 M NaCl. Fluorescence spectra of the mixture of OMUpy and 16S-rRNA were obtained from the solution. No attempt was made to eliminate dissolved oxygen in the buffer.

Fluorescence decay curve analysis

Fluorescence lifetimes were determined by a single photon counting (SPC) system (NAES-550, Horiba) equipped with a nanosecond flash lamp filled with hydrogen and with a thermal controller. Excitation light was passed through a band-path filter (half width, 40 nm; center frequency, 340 nm) and $NiSO_4 \cdot 6H_2O$ (500 g/L) aqueous solution. Sample solutions for fluorescence decay curves were the same as those for the fluorescence spectrum measurements.

Acknowledgements

We would like to thank Dr. Takashi Morii (Kyoto University, Japan) for MALDI-TOF MS analysis. This research was partially supported by a Grant-in-Aid for Scientific Research (No. 14580609, AM, TY, RI), and Grants for Regional Science and Technology Promotion (AM) from the Ministry of Education, Science, Sports and Culture of Japan.

References and Notes

1. Matveeva, O.; Felden, B.; Tsodikov, A.; Johnston, J.; Monia, B. P.; Atkins, J. F.; Gesteland, R. F.; Freier, S. M. *Nat. Biotechnol.* **1998**, *16*, 1374.
2. Vickers, T. A.; Ecker, D. J. *Nucleic Acids Res.* **1992**, *20*, 3945.
3. Milner, N.; Mir, K. U.; Southern, E. M. *Nat. Biotechnol.* **1997**, *15*, 537.
4. Sohail, M.; Akhtar, S.; Southern, E. M. *RNA* **1999**, *5*, 646.
5. Freier, S. M.; Kierzek, R.; Jaeger, J. A.; Sugimoto, N.; Caruthers, M. H.; Neilson, T.; Turner, D. H. *Proc. Natl. Acad. Sci. U.S.A.* **1986**, *83*, 9373.
6. Walter, A. E.; Turner, D. H.; Kim, J.; Lyttle, M. H.; Mûller, P.; Mathews, D. H.; Zuker, M. *Proc. Natl. Acad. Sci. U.S.A.* **1994**, *91*, 9218.
7. Chen, J.; Le, S.; Maizel, J. V. *Nucleic Acids Res.* **2000**, *28*, 991.
8. Ota, N.; Hirano, K.; Warashina, M.; Andrus, A.; Mullah, B.; Hatanaka, K.; Taira, K. *Nucleic Acids Res.* **1998**, *26*, 735.
9. Piatek, A. S.; Tyagi, S.; Pol, A. C.; Telenti, A.; Miller, L. P.; Kramer, F. R.; Alland, D. *Nat. Biotechnol.* **1998**, *16*, 359.
10. Murakami, A.; Nagahara, S.; Nakaura, M.; Uematsu, H.; Mukae, M.; Makino, K. *Nucleic Acids Symposium Series* **1990**, *22*, 27.
11. Ebata, K.; Masuko, M.; Ohtani, H.; Kashiwasake-Jibu, M. *Photochem. Photobiol.* **1995**, *62*, 836.
12. Lewis, F. D.; Zhang, Y.; Letsinger, R. L. *J. Am. Chem. Soc.* **1997**, *119*, 5451.
13. Yamana, K.; Takei, M.; Nakano, H. *Tetrahedron Lett.* **1997**, *38*, 6051.
14. Paris, P. L.; Langenhan, J. M.; Kool, E. T. *Nucleic Acids Res.* **1998**, *26*, 3789.

15. Kostenko, E.; Dobrikov, M.; Pyshnyi, D.; Petyuk, V.; Komarva, N.; Vlassov, V.; Zenkova, M. *Nucleic Acids Res*. **2001**, *29*, 3611.
16. Bernacchi, S.; Mély, Y. *Nucleic Acids Res*. **2001**, *29*, e62.
17. Yamana, K.; Iwase, R.; Furutani, S.; Tsuchida, H.; Zako, H.; Yamaoka, T.; Murakami, A. *Nucleic Acids Res*. **1999**, *27*, 2387.
18. Mahara, A.; Iwase, R.; Sakamoto, T.; Yamana, K.; Yamaoka, T.; Murakami, A. *Angew. Chem., Int. Ed*. **2002**, *19*, 3648.
19. Noller, H. F. *Ann. Rev. Biochem*. **1984**, *53*, 119.
20. Cate, J. H.; Yusupoc, M. M.; Yusupova, G. Z.; Earnest, T. N.; Noller, H. F. *Science* **1999**, *285*, 2095.
21. Clemons, W. M., Jr.; May, J. L. C.; Wimberly, B. T.; McCutcheon, J. P.; Capel, M. S.; Ramakrishnan, V. *Nature* **1999**, *400*, 833.
22. Yamana, K.; Zako, H.; Asazuma, K.; Iwase, R.; Nakano, H.; Murakami, A. *Angew. Chem., Int. Ed*. **2001**, *40*, 1104.
23. Cummins, L. L.; Owens, S. R.; Risen, L. M.; Lesnik, E. A.; Freier, S. M.; McGee, D.; Guinosso, C. J.; Cook, P. D. *Nucleic Acids Res*. **1995**, *23*, 2019.
24. Majlessi, M.; Nelson, N. C.; Becker, M. M. *Nucleic Acids Res*. **1998**, *26*, 2224.
25. Blommers, M. J.; Pieles, U.; Mesmaeker, A. D. *Nucleic Acids Res*. **1994**, *22*, 4187.
26. Pradhan, P.; Jernström, B.; Seidel, A.; Nordén, B.; Gräslund, A. *Biochemistry* **1998**, *37*, 4664.
27. Nakajima, A. *Bull. Chem. Soc. Jpn*. **1971**, *44*, 3272.